Kardiologia Polska 2017; 75, 7: 655–665; DOI: 10.5603/KP.a2017.0059 ISSN 0022–9032

ARTYKUŁ ORYGINALNY / *ORIGINAL ARTICLE*

Assessment of mitral apparatus in patients with acute inferoposterior myocardial infarction and ischaemic mitral regurgitation with two-dimensional echocardiography from anatomically correct imaging planes

Karolina Mèlinytė, Živilė Valuckienė, Renaldas Jurkevičius

Department of Cardiology, Lithuanian University of Health Sciences, Kaunas, Lithuania

Abstract

Background: Ischaemic mitral regurgitation (IMR) is associated with adverse prognosis after myocardial infarction (MI) as a result of left ventricular remodelling and geometric deformation of the mitral apparatus (MA).

Aim: The aim of this study was to assess MA from anatomically correct imaging planes in acute inferoposterior MI and IMR.

Methods: Ninety-three patients with no structural cardiac valve abnormalities and the first acute inferoposterior MI were prospectively enrolled into the study. Two-dimensional transthoracic echocardiography for MA assessment was performed within 48 h of presentation after reperfusion therapy. Based on the degree of mitral regurgitation (MR), patients were divided into either a no significant MR (NMR) group (n = 52 with no or mild, grade 0–I MR) or an IMR group (n = 41 with grade ≥ 2 MR). The control group consisted of 45 healthy individuals.

Results: Ischaemic MR was related with dilatation of the left ventricle chambers, decrease in ejection fraction, increase in mitral annulus diameter and area, and changes in subvalvular apparatus when compared with the NMR group or healthy individuals.

Conclusions: Ischaemic MR in acute inferoposterior MI is related with worse lesions in MA geometry that cause insufficiency of mitral valve function.

Key words: ischaemic mitral regurgitation, mitral apparatus, myocardial infarction, anatomically correct imaging planes

Kardiol Pol 2017; 75, 7: 655–665

INTRODUCTION

Ischaemic mitral regurgitation (IMR) is an essential and underestimated clinical problem [1]. It is an important predictor of poor prognosis with increased risk of death [2]. The normal geometry of the mitral valve apparatus becomes distorted, resulting in incomplete leaflet closure and regurgitation [3]. Extensive research has been performed to analyse the distortion of mitral apparatus (MA) in IMR and myocardial infarction (MI) using different imaging modalities [4–6]. Recent computerised tomography-based studies have shown that the conventionally used two-dimensional (2D) echocardiographic imaging planes of mitral annulus and other structures using the four-chamber view to represent the long mitral axis and parasternal long-axis views for short mitral axis measurements are anatomically incorrect [6]. Therefore, we have designed a study to investigate mitral anatomy in the first ever acute inferoposterior MI with and without IMR using conventional 2D echocardiography and anatomically aligned imaging planes.

METHODS

Study population

Patients treated for the first ever acute inferoposterior MI between January 2013 and December 2015 were prospectively enrolled into the study. Ethical approval was obtained from the regional Ethics Committee and all participants gave writ-

Address for correspondence:
Karolina Mèlinytė, MD, Department of Cardiology, Lithuanian University of Health Sciences, Eiveniu 2, LT-50009, Kaunas, Lithuania, e-mail: karolina.mlinyt652@gmail.com
Received: 25.10.2016 **Accepted:** 16.02.2017 **Available as AoP:** 15.03.2017

ten, informed consent prior to involvement. Based on mitral regurgitation (MR) degree all study patients were divided into two subgroups: a no significant MR group (NMR) (no or mild MR [grade 0–I]) or an IMR group [grade II–IV]). Fifty-two consecutive patients were included into the no-MR (NMR) group, and 41 consecutive patients with moderate or severe MR were included into the IMR group.

All patients with MI presented within 12 h of symptom onset and were treated by primary or ad-hoc percutaneous coronary intervention (PCI). Exclusion criteria were as follows: history of ischaemic heart disease (any form of angina, previous MI, coronary artery bypass surgery, or occlusive/sub-occlusive lesions in non-culprit coronary arteries suggestive of previous ischaemic events), mechanical complications of MI, suboptimal echocardiographic imaging quality, rhythm and conduction abnormalities (atrial fibrillation, atrioventricular node or His bundle branch block, implanted pacemaker), organic mitral valve disease, previously known mitral valve insufficiency, other left-sided valvular heart disease (including previous valvular heart surgery), other non-cardiac disorders that may influence myocardial contractility (diabetes mellitus, renal insufficiency), and cardiogenic shock.

Acute MI was confirmed according to European Society of Cardiology recommendations of MI definition and guidelines based on clinical symptoms, electrocardiographic findings, and cardiac enzyme abnormalities [7]. Family history of ischaemic heart disease, cardiovascular risk factors, time of symptom onset, and current treatment were recorded using a standard questionnaire. Hypertension was defined as the presence of elevated systolic (> 140 mm Hg) and/or diastolic (> 90 mm Hg) blood pressure or current use of antihypertensive drugs. A patient was considered as a smoker if he/she was currently smoking or was a smoker in the past. Dyslipidaemia was defined if any of the following criteria were present: serum total cholesterol ≥ 5.2 mmol/L, low-density lipoproteins > 2.6 mmol/L, triglycerides ≥ 1.7 mmol/L, or current use of statin medication [8].

Patients were consented and enrolled into the study after routine transthoracic echocardiogram, which was performed within 48 h of presentation, and reperfusion therapy as routine investigation.

Control group

The control group consisted of 45 healthy, age-matched, non-obese individuals with no history of ischaemic heart disease or other non-cardiac disorders that might have affected myocardial contractility (arterial hypertension, renal failure, or diabetes mellitus). They all had normal electrocardiograms and no structural or functional cardiac abnormalities detectable by echocardiography.

Coronary angiography data interpretation

Coronary angiography data were analysed and interpreted by one experienced interventional cardiologist. Coronary dominance was defined according to the artery that supplied the posterior descending artery (PDA) and labelled as right (if the PDA originated from the right coronary artery), left (if the PDA originated from the left circumflex coronary artery), or balanced (if the PDA branches originated from both right and left circumflex coronary arteries). Coronary blood flow was assessed by Thrombolysis In Myocardial Infarction (TIMI) grading (0 — no antegrade flow; 1 — weak contrast penetration beyond occlusion; 2 — slow flow; 3 — normal flow in the coronary artery) [9]. Collateral development to the culprit artery was quantified according to Rentrop classification [10].

Echocardiography

Two-dimensional echocardiography was performed within 48 h of presentation and reperfusion therapy PCI by one experienced physician-echocardiographer. Patients were imaged in the left lateral decubitus position using a GE Vivid 7 echocardiography system. Standard images were obtained using a 3.5-MHz transducer. The frame rates of acquired images were between 82 and 95 frames/s.

Two-dimensional echocardiography was used to assess conventional echocardiographic parameters. Left ventricular (LV) end-diastolic diameter (LVEDD), LV end-systolic diameter (LVESD), and left atrium (LA) diameter were measured from parasternal long-axis view (LVEDD at end-diastole, LVESD and LA diameters at end-systole). Left atrial volume (LAV) was calculated using the apical biplane area-length method, and LAV was indexed to body surface area. The LV long axis was obtained from the longest distance between the centre of the mitral annulus and the endocardial apex on the four-chamber view. LV and right ventricle (RV) diameters were measured from apical four-chamber view at mid-ventricular level at end-diastole and end-systole. For 2D cardiac morphometric measurements end-diastole was defined as the cardiac cycle frame when the LV or RV internal diameter was largest, and end-systole as the frame when the LV or RV cavity was smallest. LV end-diastolic volume (LVEDV) and LV end-systolic volume (LVESV), LV ejection fraction (LVEF) were measured from the apical four- and two-chamber views and calculated by Simpson's biplane method, following manual delineation of the endocardial border in the largest (end-diastolic) and smallest (end-systolic) boundary. LVEF (%) was estimated by the following formula: (LVEDV – LVESV) / LVEDV × 100%. Myocardial mass (MM) was calculated by the Devereux formula [11]. Myocardial mass index (MMI) was calculated by dividing MM (g) by body surface area (m^2). Tricuspid annular plane systolic excursion (TAPSE) was used to assess RV systolic function in 2D M-mode echocardiograms from the four-chamber view, positioning the cursor on the lateral tricuspid annulus near the free RV wall.

Mitral regurgitation was quantified by standard PISA method according to the recommendations provided by the European Association of Cardiovascular Imaging [12] and reported as: none (grade 0), mild (grade I, regurgitant orifice area

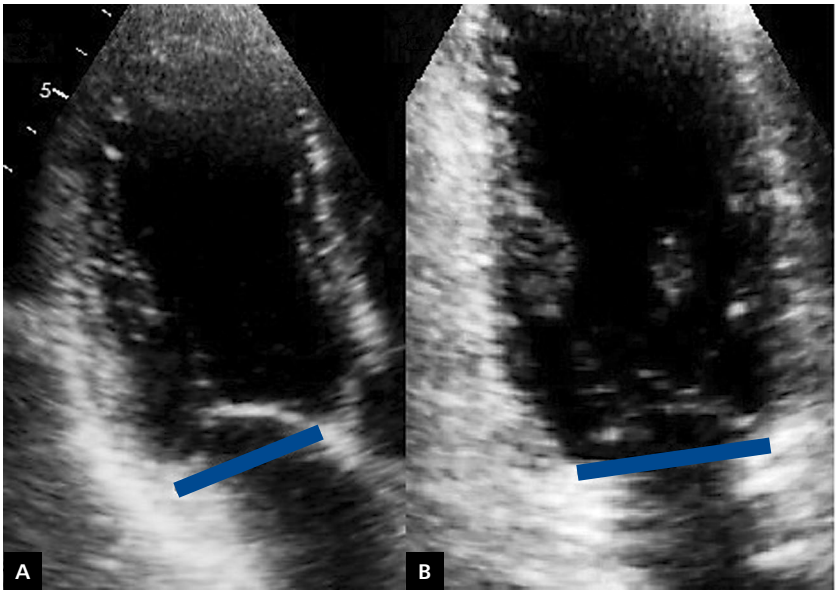

Figure 1. Models of transthoracic echocardiographic views used to visualise the mitral annulus; **A.** Anterior-posterior diameter; **B.** Commissure-commissure diameter

[ROA] < 0.2 cm^2), moderate (grade II, ROA 0.2–0.3 cm^2), or severe (grade III–IV, ROA ≥ 0.3 cm^2 or ≥ 0.4 cm^2, respectively).

Measurements of the MA

All MA measurements were obtained from 2D echocardiographic views by one experienced echocardiographer. All the parameters were indexed to body surface area to standardise values. Mitral annular dimensions were obtained from apical long axis view (three-chamber, antero-posterior [AP] diameter) (Fig. 1A) and apical bicommissural view (intercommissural [IC] diameter) when P1-A2-P3 mitral leaflet scallops were visualised as the distance between opposite sites of leaflet insertion to the fibrotic annulus (Fig. 1B). The echocardiographic views were obtained in end-systole.

Mitral annulus area (MAA) was calculated in end-diastole and end-systole using the formula of an ellipse: MAA = $\pi \times r1 \times r2/4$ — where r1 and r2 were AP and IC mitral annular dimensions, respectively [4]. Tenting height was measured as the distance between the coaptation point of the mitral leaflets and the annular plane (reflected by the line connecting the contralateral leaflet insertion points to the annulus) of the mitral valve in systole from the apical long-axis (three-chamber) view — Figure 2 (black line). The mitral leaflet tenting area was derived between the leaflets and the line connecting the annular hinge points in the apical three-chamber view in systole (Fig. 2; blue trapeze). Anterior mitral leaflet (AML) and posterior mitral leaflet (PML) lengths were measured in diastole from the apical three-chamber view. Leaflet length was designated as the distance from the most distal extent of the anterior leaflet to its insertion into the anterior mitral annulus and the most distal extent of posterior leaflet into the posterior mitral annulus (Fig. 3). The posteromedial papillary muscle (PMPM) displacement was quantified as the distance in systole between these points in the apical three-chamber view (Fig. 4): the PMPM tip and contralateral anterior mitral annulus (the site of anterior leaflet insertion; blue line A-B); the PMPM tip and leaflets coaptation point (blue line A-C); and the PMPM tip and mitral annulus plane distance (blue line A-D). Interpapillary muscle distance (IPMD) in systole was measured between the endocardial borders of the papillary muscle heads from the parasternal short-axis mid-ventricular level view with both papillary muscles visible in cross-section (Fig. 5).

Statistical analysis

Continuous variables were expressed as means ± standard deviations (SD). Differences in variables between the three groups were assessed by the one-way ANNOVA t-test. Categorical variables are presented as absolute numbers and percentages and were compared using χ^2 test. The Kolmogorov-Smirnov test was used to detect the normality of distribution of the data. Student's t-test was used to compare normally distributed variables, and the Mann-Whitney U test was used for abnormally distributed variables among groups. Pearson's correlation coefficient (r) was used to evaluate links between LV and MA geometry. Multiple linear regression analysis, including all significant parameters identified by univariate analysis (at a significance level of $p < 0.10$), was used to evaluate the most important MA determinants of IMR. A p value < 0.05 was considered statistically significant.

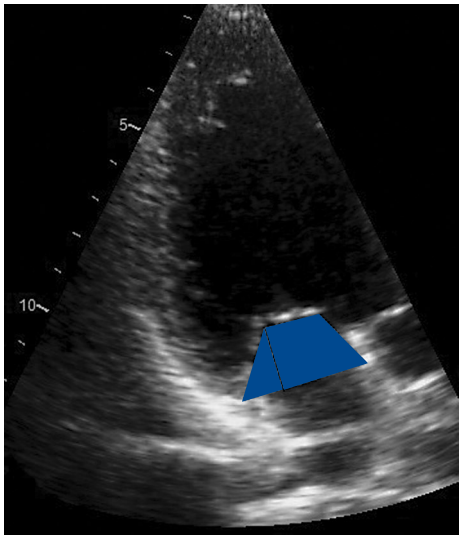

Figure 2. Illustration represents mitral leaflet tenting area (blue figure) and coaptation height (black line)

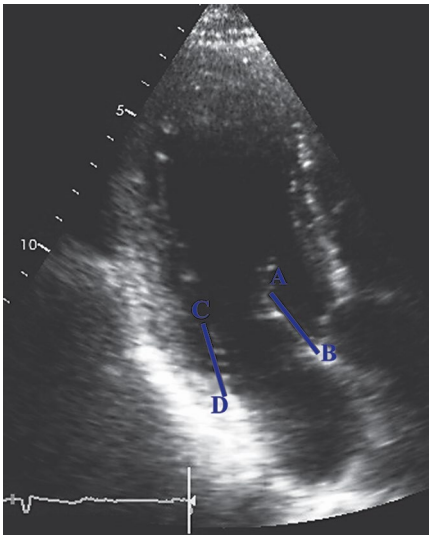

Figure 3. Illustration shows anterior (A–B blue line) and posterior (C–D blue line) mitral leaflet length

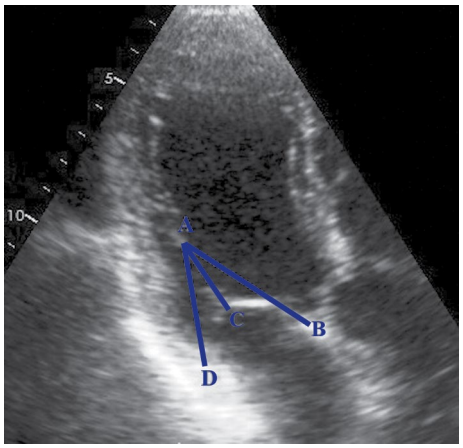

Figure 4. Illustration shows the apical displacement of posteromedial papillary muscle in the apical three-chamber view (blue lines)

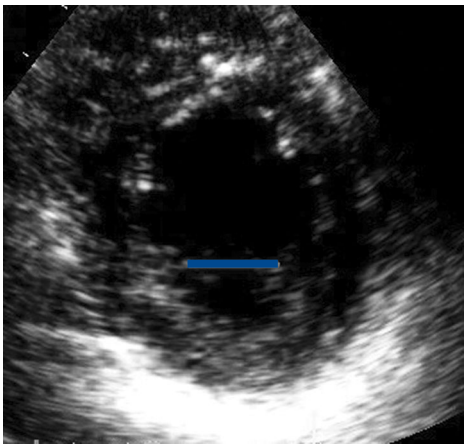

Figure 5. Illustration represents parasternal short-axis mid-ventricular level view in systole with papillary muscle bodies in cross-section

RESULTS

Table 1 represents the clinical characteristics of the study groups. The average age in the NMR and IMR groups was similar ($p = 0.998$), and members of these groups were more likely to be male, compared with the healthy group. Dyslipidaemia, smoking, and arterial hypertension were less likely to be present in the control group, when compared to the NMR or IMR group ($p < 0.05$). There was no statistically significant association found between the presence of MR and Killip heart failure class distribution ($p = 0.348$), heart rate upon admission ($p = 0.382$), and diastolic blood pressure ($p = 0.086$). Patients in the IMR group had higher systolic blood pressure upon presentation ($p = 0.004$). The biochemical profile between NMR and IMR groups was similar.

All patients had undergone coronary angiography (Table 2). There was a statistically significant difference between the localisations of the dominant artery. Right coronary artery was significantly more dominant in the group with no MR when compared to the IMR group. Balanced coronary dominance was more detectable in the IMR group. Ramus circumflexus lesion was found to be strongly associated with the presence of IMR ($p = 0.002$). There was no significant relation in the distribution of both study groups between the TIMI grade before ($p = 0.100$) and after ($p = 0.140$) the PCI. There was no significant relation between the presence of distal embolisation during PCI and residual stenosis in the MI area in the MR groups. More developed collateral flow was noticed in the IMR group when compared to the NMR group ($p = 0.023$).

Table 1. Demographic and clinical characteristics

Data	Control group (I) N = 45	NMR group (II) N = 52	IMR group (III) N = 41	P		
				I vs. II	I vs. III	II vs. III
Age [years]	57.3 ± 6.1	61.3 ± 11.6	61.5 ± 11.4	0.2	0.08	0.998
Sex:				0.003	0.525	0.025
Female	23 (51.1%)	11 (21.2%)	18 (43.9%)			
Male	22 (48.9%)	41(78.8%)	23 (56.1%)			
Dyslipidaemia	13 (14.6%)	41 (46.1%)	35 (39.3%)	< 0.001	< 0.001	0.590
Smoking	13 (19.4%)	32 (47.8%)	22 (32.8%)	0.002	0.028	0.527
Hypertension	7 (10.6%)	30 (45.5%)	29 (43.9%)	< 0.001	< 0.001	0.278
Body surface area [m^2]	1.9 ± 0.2	1.9 ± 0.2	1.9 ± 0.1	0.446	0.999	0.444
Killip heart failure class distribution (within MR groups):					0.348	
I	30 (63.8%)	17 (36.2%)				
II	17 (44.7%)	21 (55.3%)				
III	2 (66.7%)	1 (33.3%)				
IV	3 (60%)	2 (40%)				
Vital parameters:						
Heart rate upon admission [bpm]		71.1 ± 14,1	67.6 ± 13,4		0.382	
Systolic blood pressure [mm Hg]		130.0 ± 22.5	145.0 ± 25.4		0.004	
Diastolic blood pressure [mm Hg]		77.0 ± 12.7	81.8 ± 13.8		0.086	
Biochemical profile:						
Total cholesterol [mg/dL]		203.6 ± 51.6	211.4 ± 48.2		0.463	
Triglycerides [mg/dL]		128.1 ± 76.0	126.8 ± 69.1		0.931	
HDL [mg/dL]		43.0 ± 9.8	44.2 ± 13.3		0.611	
LDL [mg/dL]		132.2 ± 42.0	140.0 ± 40.2		0.377	
Peak troponin I [μg/L]		44.0 ± 56.8	73.9 ± 108.4		0.163	
NT-proBNP [ng/L]		593.3 ± 338.0	604.04 ± 360.1		0.785	
CRP [mg/L]		12.9 ± 26.0	13.1 ± 16.5		0.976	
Random plasma glucose on admission [mg/dL]		122.1 ± 29.9	123.9 ± 34.8		0.791	

NMR — no mitral regurgitation; IMR — ischaemic mitral regurgitation; MR — mitral regurgitation; HDL — high-density lipoproteins; LDL — low-density lipoproteins; NT-proBNP — N-terminal pro-B-type natriuretic peptide; CRP — C reactive protein

Table 3 represents distribution of echocardiographic parameters between the study groups. All LV cavity diameters were significantly higher in both MI groups ($p < 0.05$). LA diameter was larger in the NMR and IMR groups when compared with the control group ($p < 0.001$). A significant decrease of LVEF was observed either in the NMR or IMR group when compared to the control group ($p < 0.001$). LVESV, LVESV index were higher in both MI groups ($p < 0.001$). LAV index, and LV and RV diameters were significantly higher in the moderate-to-severe MR when compared with controls. TAPSE measurements were similar in all study groups ($p > 0.05$).

Characteristics of MA are presented in Figure 6. Study groups with MI had significantly larger MAA, greater MA AP diameter and tethering height ($p < 0.05$), compared to the control group. It was noticed that these parameters were greater in the IMR group when compared to the NMR group. Mitral annulus IC distance was similar between the control and NMR groups ($p = 0.619$, $p > 0.05$) but significantly higher in the IMR group ($p = 0.015$, $p < 0.05$). There was a statistically significant difference in mitral valve tenting area between the control and IMR groups ($p < 0.05$). AML was similar in healthy individuals and in the NMR groups, but longer in patients with IMR. There was no difference in PML length between the control and IMR groups and both study MI groups ($p > 0.05$). PMPM — anterior mitral annulus and PMPM — coaptation point distances were greater in both study groups compared to healthy individuals ($p < 0.05$), but there was no difference in PMPM — coaptation point distance between NMR and IMR groups ($p > 0.05$). PMPM — MA distance was similar between all study groups ($p > 0.05$). However, IPMD was higher in both MI groups when compared to the control group ($p < 0.05$).

Table 2. Angiographic data

Data	NMR (n = 52)	IMR (n = 41)	p
Coronary dominance:			0.025
LCA	4 (40%)[a]	28 (37.3%)[b]	
RCA	6 (60%)[a]	1 (14.3%)[a]	
Balanced	47 (62.7%)[a]	6 (85.7%)[b]	
Culprit artery:			
RCx	11 (34.4%)	21 (65.6%)	0.002
RCA	46 (59.7%)	31 (40.3%)	0.085
TIMI flow before PCI:			0.100
Grade 0	26 (50%)[a]	26 (50%)[a]	
Grade 1	0 (0%)[a]	2 (100%)[a]	
Grade 2	11 (64.7%)[a]	6 (35.3%)[a]	
Grade 3	14 (73.7%)[a]	5 (26.3%)[a]	
TIMI flow after PCI:			0.140
Grade 0	0 (0.%)[a]	3 (100%)[b]	
Grade 1	0 (0%)[a]	1 (100%)[a]	
Grade 2	3 (60%)[a]	2 (40%)[a]	
Grade 3	48 (59.3%)[a]	33 (40.7%)[a]	
Distal embolisation during PCI	12 (70.6%)	5 (29.4%)	0.224
Residual stenosis in MI area	9 (45.0%)	11 (55.0%)	0.174
Residual stenosis in other MV area	15 (45.5%)	18 (54.5%)	0.094
Residual stenosis in small vessels	19 (51.4%)	18 (48.6%)	0.297
Collateral flow:			0.023
0	36 (65.5%)[a]	19 (34.5%)[b]	
1	8 (61.5%)[a]	5 (38.5%)[a]	
2	3 (50.0%)[a]	3 (50.0%)[a]	
3	4 (23.5%)[a]	13 (76.5%)[b]	

[a,b]Difference is statistically significant between different letters, and insignificant between the same letters. NMR — no mitral regurgitation; IMR — ischaemic mitral regurgitation; LCA — left coronary artery; RCA — right coronary artery; RCx — ramus circumflexus; TIMI — Thrombolysis In Myocardial Infarction coronary flow grade; PCI — percutaneous coronary intervention; MV — main vessels; MI — myocardial infarction

Figure 7 shows the most significant correlations between LV size and changes of MA geometry parameters. Expansion of LV short axis in systole was related with mitral annulus AP diameter increase in systole ($r = 0.582$, $p < 0.001$). LV long axis at the same cardiac cycle showed the most significant correlation with posteromedial papillary muscle — anterior mitral annulus distance ($r = 0.546$, $p < 0.001$). This finding shows that PMPM displacement after MI is related with enlargement of LV long axis. LV systolic volume and systolic diameter had the strongest relationship with mitral annulus area and AP diameter, respectively (LV diastolic volume and diameter were correlated with the same parameters of MA but not as strongly as in systole).

Table 4 represents results of linear logistic regression analysis with MR degree as a dependent variable and MA parameters as independent variables. Of all MA parameters, AP diameter, tenting height, posteromedial papillary muscle displacement, and interpapillary muscle distance were found to be the most significant predictors of IMR.

DISCUSSION

Moderate or severe MR is a disease that is found in 1.7% of the general population, 6.4% of patients aged 65–74 years, and 9.3% of those aged > 75 years [13, 14]. The results of many studies demonstrate higher incidence of IMR in inferior compared with anterior MI. Inferior basal LV remodelling causes more severe geometric alterations in the mitral valve apparatus with greater displacement of PMPM [15–19]. Based on these findings, in this study mitral valve geometry was assessed in patients with inferoposterior MI. Our analysis and others have previously shown that IMR after acute MI is associated with worse LV function, greater LV enlargement, and MA parameter deformation [19, 20]. This study is one of the first that investigates MA geometry in patients with no or severe MR in acute phase of inferoposterior MI from anatomically correct imaging planes.

The mitral annulus after MI undergoes a number of structural changes in IMR, becoming larger and flatter [5, 20, 21]. An increase in size causes the effacement of the mitral

Table 3. Conventional echocardiographic parameters

Variable	Control group (I group; n = 45)	NMR (II group; n = 52)	IMR (III group; n = 41)	p		
				I vs. II	I vs. III	II vs. III
LVEDD [mm]	45.8 ± 5.1	50.5 ± 5.5	54.2 ± 5.3	< 0.001	< 0.001	0.003
LVEDDi [mm/m^2]	23.7 ± 2.3	25.5 ± 2,5	28.2 ± 3.4	0.006	< 0.001	< 0.001
LVESD [mm]	31.9 ± 5.3	38.4 ± 6.9	42.5 ± 5.8	< 0.001	< 0.001	0.005
LVESDi [mm/m^2]	16.5 ± 2.6	19.4 ± 3.3	22.1 ± 3.7	< 0.001	< 0.001	< 0.001
LA [mm]	32.3 ± 3.9	36.9 ± 4.5	38.9 ± 4.0	< 0.001	< 0.001	0.077
LAi [mm/m^2]	16.7 ± 1.7	18.7 ± 2.4	20.2 ± 2.7	< 0.001	< 0.001	0.006
LVEF [%]	61.84 ± 5.2	51.4 ± 7.0	46.9 ± 7.5	< 0.001	< 0.001	0.002
LVEDV [mL]	100.7 ± 26.1	108.3 ± 31.3	121.9 ± 28.5	0.597	0.003	0.077
LVEDVi [mL/m^2]	51.5 ± 9.4	53.9 ± 12.9	63.0 ± 13.5	0.590	< 0.001	0.001
LVESV [mL]	38.0 ± 12.7	53.3 ± 19.3	65.3 ± 21.4	< 0.001	< 0.001	0.006
LVESVi [mL/m^2]	19.4 ± 5.1	26.4 ± 8.3	33.8 ± 10.9	< 0.001	< 0.001	< 0.001
LAVI [mL/m^2]	24.3 ± 5.4	28.6 ± 7.2	36.4 ± 9.2	0.052	< 0.001	0.039
LVLA (S) [mm/m^2]	32.4 ± 3.2	34.8 ± 4.3	37.3 ± 4.4	0.015	< 0.001	0.012
LVSA (S) [mm/m^2]	16.8 ± 2.7	18.3 ± 2.2	20.2 ± 3.1	0.017	<0.001	0.004
RVSA (D) [mm/m^2]	13.5 ± 2.0	14.1 ± 2.5	15.1 ± 2.6	0.414	0.006	0.119
RVSA (S) [mm/m^2]	9.9 ± 1.6	10.8 ± 2.0	12.2 ± 2.2	0.057	< 0.001	0.006
TAPSE [mm]	22.5 ± 3.6	20.2 ± 4.0	20.1 ± 4.8	0.310	0.312	0.989
MMI [g/m^2]	74.3 ± 15.5	100.3 ± 19.8	133.6 ± 36.1	< 0.001	< 0.001	< 0.001

NMR — no significant mitral regurgitation (grade 0–I) group; IMR — ischaemic mitral regurgitation group (grade II–IV); LVEF — left ventricular ejection fraction; LVEDD — left ventricular end-diastolic diameter; LVESD — left ventricular end-systolic diameter; LVEDV — left ventricular end--diastolic volume; LVESV — left ventricular end-systolic volume; MMI — myocardial mass index; LA — left atrial diameter in systole; LAVI — left atrial volume index; LVLA — left ventricular long axis; LVSA — left ventricular short axis; RVSA — right ventricular short axis; S — end systole; D — end diastole; TAPSE — tricuspid annular plane systolic excursion

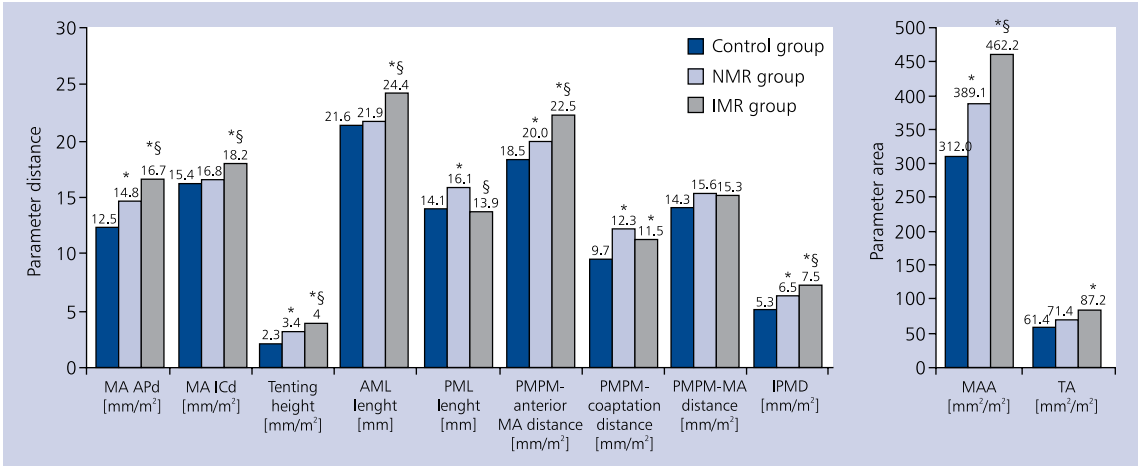

Figure 6. Mitral apparatus characteristics; *p < 0.05, compared with control group; §p < 0.05, compared with no mitral regurgitation group; MA — mitral annulus; APd — anteroposterior diameter; ICd — intercommissural diameter; AML — anterior mitral leaflet; PML — posterior mitral leaflet; MAA — mitral annular area; TA — tenting area; PMPM — posteromedial papillary muscle; IPMD — interpapillary muscle distance; NMR — no mitral regurgitation; IMR — ischaemic mitral regurgitation

leaflets compromising coaptation length. Three-dimensional (3D) echocardiography with planimetric method can be used to evaluate MAA precisely [22, 23]. Hyodo et al. [4] elucidated which methods have similar efficiency to that of the

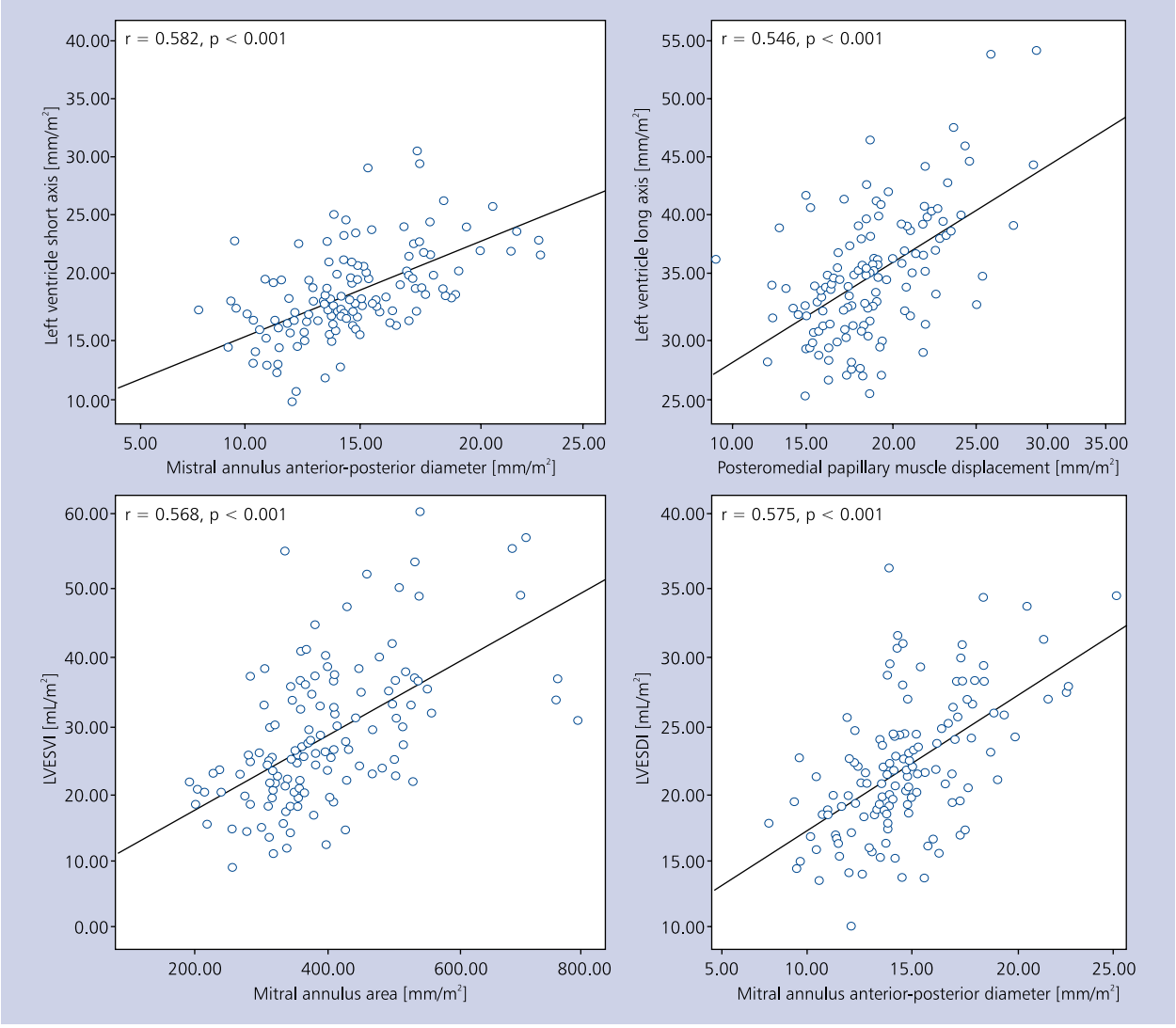

Figure 7. Left ventricle and mitral apparatus geometry correlation; LVESVI — left ventricular end-systolic volume index; LVESDI — left ventricular end-systolic diameter index

Table 4. Prognostic parameters of the mitral apparatus for ischaemic mitral regurgitation in acute inferoposterior myocardial infarction

Parameter	Standardised coefficient (β)	95% confidence interval for β	p
MA anteroposterior diameter [mm]	0.457	0.036–0.105	< 0.001
Tenting height [mm]	0.477	0.104–0.217	< 0.001
PMPM-coaptation distance [mm]	0.248	0.008–0.066	0.013
IPMD [mm]	0.185	0.012–0.079	0.009

MA — mitral annulus; PMPM — posteromedial papillary muscle; IPMD — interpapillary muscle distance

3D planimetric method for MAA measurement. AP/IC planes were found to be the most accurate method for measuring MAA without the influence of the annular shape. These results suggest that AP/IC plane measurements are the best alternative to the standard 3D planimetric MAA measurements [4]. In their study, Foster et al. [6] showed that the correct anatomic imaging planes method of mitral annulus measurement correlated very well with cardiac computed tomography. Our study has shown that AP diameter mostly correlated with MR degree when compared with IC plane.

The changes of the geometry of the subvalvular apparatus are the main determinants of the IMR, especially the papillary muscle displacement and leaflet tenting. Local remodelling of the LV displaces papillary muscles and leads to a traction on the mitral leaflets [24]. In our study the tenting height, leaflet tenting area, and PMPM displacement mostly varied in the patient group with a higher degree of IMR. These lesions are confirmed in a previous study as well [25]. But there is a difference between measurements of MA: in this study parameters are evaluated from anatomically correct imaging planes compared to other studies with conventional methods. In the present study multivariate analysis has shown that AP diameter, tenting height, posteromedial papillary muscle displacement, and interpapillary muscle distance were the main determinants of IMR.

Left ventricular remodelling after MI is the strongest factor that causes changes in mitral valve apparatus. Based on this, our results have shown that mitral annulus and papillary muscle geometry variation correlated most with the alterations of LV.

Time to reperfusion is an important factor in preservation of the myocardium. Recent studies have demonstrated the importance of collateral supply in IMR reduction [26]. Despite this, other studies have shown that collateral flow compensates for antegrade flow reduction and relieves ischaemia in stable coronary artery disease with chronic total occlusion in less than 5% of patients [27]. In our study, a large proportion of patients exhibited IMR despite well-developed collateral flow to occluded culprit artery region. Accordingly, more studies are needed to assess the impact of collateral flow on IMR on long-term follow-up.

Limitations of the study

The study samples were not large and may have been influenced by multiple exclusion criteria that are indicated at the methodology part of this study.

CONCLUSIONS

A comprehensive assessment of MA in IMR after acute inferoposterior MI provides further verification of the important role of mitral geometric deformation in the origin of IMR. It was noticed that AP diameter mostly correlated with MR degree when compared with IC plane. AP diameter, tenting height, PMPM displacement, and IPMD were found to be the most significant predictors in the development of IMR.

Conflict of interest: *none declared*

References

1. Dudzinski DM, Hung J. Echocardiographic assessment of ischemic mitral regurgitation. Cardiovasc Ultrasound. 2014; 12: 46, doi: 10.1186/1476-7120-12-46, indexed in Pubmed: 25416497.
2. Meris A, Amigoni M, Verma A, et al. Mechanisms and predictors of mitral regurgitation after high-risk myocardial infarction. J Am Soc Echocardiogr. 2012; 25(5): 535–542, doi: 10.1016/j.echo.2012.01.006, indexed in Pubmed: 22305962.
3. Silbiger JJ. Mechanistic insights into ischemic mitral regurgitation: echocardiographic and surgical implications. J Am Soc Echocardiogr. 2011; 24(7): 707–719, doi: 10.1016/j.echo.2011.04.001, indexed in Pubmed: 21592725.
4. Hyodo E, Iwata S, Tugcu A, et al. Accurate measurement of mitral annular area by using single and biplane linear measurements: comparison of conventional methods with the three-dimensional planimetric method. Eur Heart J Cardiovasc Imaging. 2012; 13(7): 605–611, doi: 10.1093/ejechocard/jer300, indexed in Pubmed: 22210708.
5. Watanabe N, Ogasawara Y, Yamaura Y, et al. Mitral annulus flattens in ischemic mitral regurgitation: geometric differences between inferior and anterior myocardial infarction: a real-time 3-dimensional echocardiographic study. Circulation. 2005; 112(9 Suppl): I458–I462, doi: 10.1161/CIRCULATIONAHA.104.524595, indexed in Pubmed: 16159863.
6. Foster GP, Dunn AK, Abraham S, et al. Accurate measurement of mitral annular dimensions by echocardiography: importance of correctly aligned imaging planes and anatomic landmarks. J Am Soc Echocardiogr. 2009; 22(5): 458–463, doi: 10.1016/j.echo.2009.02.008, indexed in Pubmed: 19359141.
7. Thygesen K, Alpert JS, Jaffe AS, et al. Third universal definition of myocardial infarction. Eur Heart J. 2012; 33: 2551––2567, doi: 10.1093/eurheartj/ehs184, indexed in Pubmed: 22923432.
8. Catapano A, Reiner Ž, De Backer G, et al. SC/EAS Guidelines for the management of dyslipidaemias. The Task Force for the management of dyslipidaemias of the European Society of Cardiology (ESC) and the European Atherosclerosis Society (EAS). Atherosclerosis. 2011; 217(1): 3–46, doi: 10.1016/j.atherosclerosis.2011.06.028.
9. TIMI Study Group. The Thrombolysis in Myocardial Infarction (TIMI) trial. Phase I findings. N Engl J Med. 1985; 312(14): 932–936, doi: 10.1056/NEJM198504043121437, indexed in Pubmed: 4038784.
10. Rentrop KP, Cohen M, Blanke H, et al. Changes in collateral channel filling immediately after controlled coronary artery occlusion by an angioplasty balloon in human subjects. J Am Coll Cardiol. 1985; 5(3): 587–592, indexed in Pubmed: 3156171.
11. Schiller NB, Shah PM, Crawford M, et al. Recommendations for quantitation of the left ventricle by two-dimensional echocardiography. American Society of Echocardiography Committee on Standards, Subcommittee on Quantitation of Two-Dimensional Echocardiograms. J Am Soc Echocardiogr. 1989; 2(5): 358–367, indexed in Pubmed: 2698218.
12. Lancellotti P, Tribouilloy C, Hagendorff A, et al. Recommendations for the echocardiographic assessment of native valvular regurgitation: an executive summary from the European Association of Cardiovascular Imaging. Eur Heart J Cardiovasc Imaging. 2013; 14(7): 611–644, doi: 10.1093/ehjci/jet105, indexed in Pubmed: 23733442.
13. Nkomo VT, Gardin JM, Skelton TN, et al. Burden of valvular heart diseases: a population-based study. Lancet. 2006; 368(9540): 1005–1011, doi: 10.1016/S0140-6736(06)69208-8, indexed in Pubmed: 16980116.
14. Iung B, Vahanian A. Epidemiology of valvular heart disease in the adult. Nat Rev Cardiol. 2011; 8(3): 162–172, doi: 10.1038/nrcardio.2010.202, indexed in Pubmed: 21263455.
15. Agricola E, Oppizzi M, Pisani M, et al. Ischemic mitral regurgitation: Mechanisms and echocardiographic classification. Eur Heart J, 2008; 9: 207–221, doi: 10.1016/j.euje.2007.03.034.
16. Izumi S, Miyatake K, Beppu S, et al. Mechanism of mitral regurgitation in patients with myocardial infarction: a study using real-time two-dimensional Doppler flow imaging and echocardiography. Circulation. 1987; 76(4): 777–785, indexed in Pubmed: 3652421.
17. Leor J, Feinberg MS, Vered Z, et al. Effect of thrombolytic therapy on the evolution of significant mitral regurgitation in patients

with a first inferior myocardial infarction. J Am Coll Cardiol. 1993; 21(7): 1661–1666, indexed in Pubmed: 8496534.
18. Roberts R, Morris D, Pratt CM. Pathophysiology, recognition, and treatment of acute myocardial infarction and its complications. In: Schlant RC, Alexander RW, editors. McGraw-Hill Inc, New York 1994: 1115.
19. Kumanohoso T, Otsuji Y, Yoshifuku S, et al. Mechanism of higher incidence of ischemic mitral regurgitation in patients with inferior myocardial infarction: quantitative analysis of left ventricular and mitral valve geometry in 103 patients with prior myocardial infarction. J Thorac Cardiovasc Surg. 2003; 125(1): 135–143, doi: 10.1067/mva.2003.78, indexed in Pubmed: 12538997.
20. Mihalatos DG, Mathew ST, Gopal AS, et al. Relationship of mitral annular remodeling to severity of chronic mitral regurgitation. J Am Soc Echocardiogr. 2006; 19(1): 76–82, doi: 10.1016/j.echo.2005.05.010, indexed in Pubmed: 16423673.
21. De Simone R, Wolf I, Mottl-Link S, et al. A clinical study of annular geometry and dynamics in patients with ischemic mitral regurgitation: new insights into asymmetrical ring annuloplasty. Eur J Cardiothorac Surg. 2006; 29(3): 355–361, doi: 10.1016/j.ejcts.2005.12.034, indexed in Pubmed: 16439153.
22. Suri RM, Grewal J, Mankad S, et al. Is the anterior intertrigonal distance increased in patients with mitral regurgitation due to leaflet prolapse? Ann Thorac Surg. 2009; 88(4): 1202–1208, doi: 10.1016/j.athoracsur.2009.04.112, indexed in Pubmed: 19766808.
23. Kovalova S, Necas J. RT-3D TEE: characteristics of mitral annulus using mitral valve quantification (MVQ) program. Echocardiography. 2011; 28(4): 461–467, doi: 10.1111/j.1540-8175.2010.01340.x, indexed in Pubmed: 21175781.
24. Iung B. Management of ischaemic mitral regurgitation. Heart. 2003; 89(4): 459–464, doi: 10.1136/heart.89.4.459.
25. Sadeghpour A, Abtahi F, Kiavar M, et al. Echocardiographic evaluation of mitral geometry in functional mitral regurgitation. J Cardiothorac Surg. 2008; 3: 54, doi: 10.1186/1749-8090-3-54, indexed in Pubmed: 18840276.
26. Weinstein JM, Kidman G, Ilia R. Collateral-dependent ischemic mitral regurgitation. J Invasive Cardiol. 2014; 26(3): E27–E28, indexed in Pubmed: 24610511.
27. Traupe T, Gloekler S, de Marchi SF, et al. Assessment of the human coronary collateral circulation. Circulation. 2010; 122(12): 1210–1220, doi: 10.1161/CIRCULATIONAHA.109.930651, indexed in Pubmed: 20855668.

Cite this article as: Mèlinytè K, Valuckienè Ž, Jurkevičius R. Assessment of mitral apparatus in patients with acute inferoposterior myocardial infarction and ischaemic mitral regurgitation with two-dimensional echocardiography from anatomically correct imaging planes. Kardiol Pol. 2017; 75(7): 655–665, doi: 10.5603/KP.a2017.0059.

Ocena aparatu zastawkowego zastawki mitralnej u chorych z ostrym zawałem ściany tylno-dolnej serca i niedokrwienną niedomykalnością zastawki mitralnej na podstawie echokardiografii dwuwymiarowej w odpowiednich płaszczyznach obrazowania anatomicznego

Karolina Mèlinyte, Živilè Valuckiènè, Renaldas Jurkevičius

Department of Cardiology, Lithuanian University of Health Sciences, Kaunas, Litwa

Streszczenie

Wstęp: Niedomykalność niedokrwienna zastawki mitralnej (IMR) w następstwie remodelingu lewej komory i geometrycznej deformacji aparatu zastawkowego (MA) wiąże się z niekorzystnym rokowaniem po zawale serca.

Cel: Badanie przeprowadzono w celu oceny MA na podstawie badania echokardiograficznego w odpowiednich płaszczyznach obrazowania anatomicznego u chorych z ostrym zawałem tylno-dolnej ściany serca i niedomykalnością zastawki mitralnej.

Metody: Do badania włączono prospektywnie 93 chorych bez strukturalnych zmian zastawek serca, u których stwierdzono po raz pierwszy w życiu zawał ściany tylno-dolnej. U pacjentów wykonano dwuwymiarową echokardiografię przezklatkową w celu oceny aparatu zastawkowego w ciągu 48 h od zgłoszenia się chorego po leczeniu reperfuzyjnym. Na podstawie stopnia niedomykalności zastawki mitralnej (MR) chorych podzielono na dwie grupy: osoby bez istotnej MR (NMR; n = 52; bez cech niedomykalności lub niedomykaloność łagodna [stopień 0–I] MR) oraz osoby z niedokrwienną MR (IMR; n = 41, z MR ≥ 2 stopnia). Grupę kontrolną stanowiło 45 zdrowych osób.

Wyniki: Niedomykalność niedokrwienna zastawki mitralnej wiązała się z poszerzeniem lewej komory, obniżeniem frakcji wyrzutowej, zwiększeniem średnicy i powierzchni pierścienia zastawki mitralnej oraz zmianami w obrębie aparatu podzastawkowego w porównaniu z grupą NMR i osobami zdrowymi.

Wnioski: Niedomykalność niedokrwienna zastawki mitralnej w ostrym zawale ściany tylno-dolnej wiąże się z większymi zmianami geometrii MA powodującymi nieprawidłową czynność zastawki mitralnej.

Słowa kluczowe: niedomykalność niedokrwienna zastawki mitralnej, aparat zastawkowy, zawał serca, odpowiednie płaszczyzny obrazowania anatomicznego

Kardiol Pol 2017; 75, 7: 655–665

Adres do korespondencji:
Karolina Mèlinytè, MD, Department of Cardiology, Lithuanian University of Health Sciences, Eiveniu 2, LT-50009, Kaunas, Lithuania, e-mail: karolina.mlinyt652@gmail.com
Praca wpłynęła: 25.10.2016 r. **Zaakceptowana do druku:** 16.02.2017 r. **Data publikacji AoP:** 15.03.2017 r.